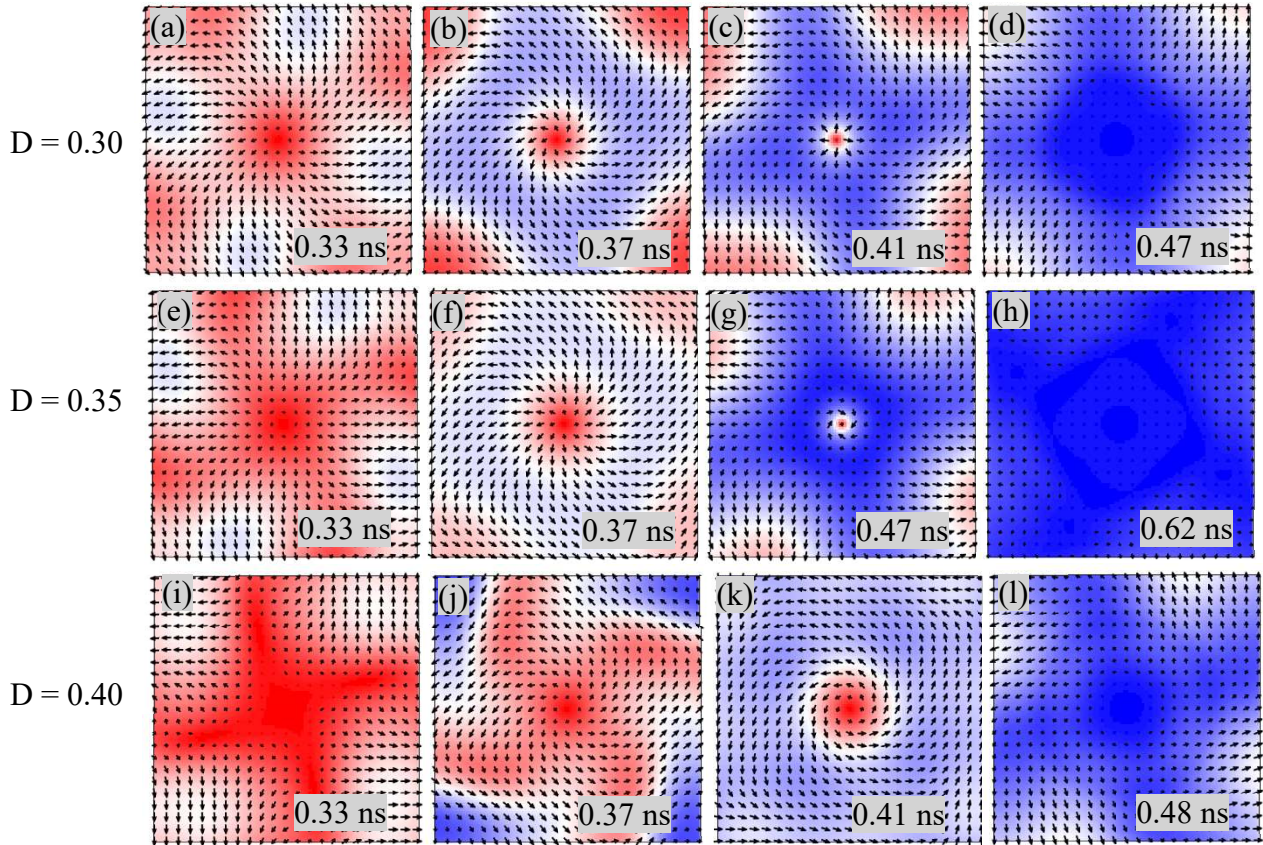
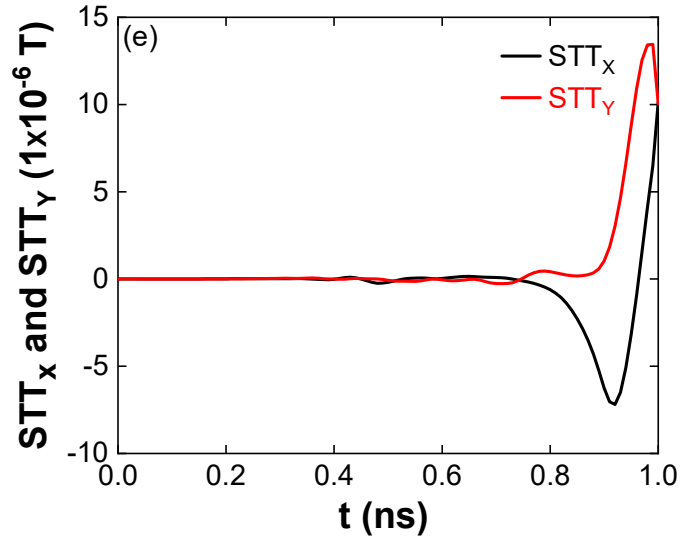
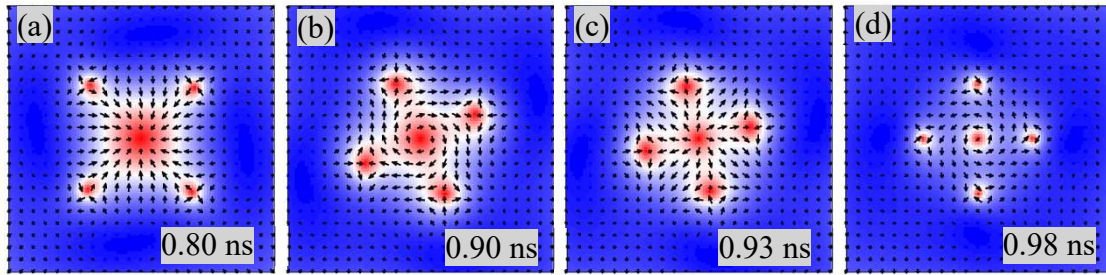


**Isolated skyrmion, skyrmion lattice, and antiskyrmion lattice creation through magnetization reversal in Co/Pd nanostructure**

**Supplementary Figures**



**Fig. 1:** Captured spin states for  $J = 4 \times 10^{11} \text{ A/m}^2$  and 1.0 ns pulse width. Red colour indicates the magnetization along the  $+z$  direction, blue along the  $-z$  direction and white in the plane. **(a) – (d)** For  $D = 0.30 \text{ mJ/m}^2$  and **(e) – (h)** are for  $D = 0.35 \text{ mJ/m}^2$ , the skyrmion formation from the edge centre to annihilation. **(i) – (j)** For  $D = 0.40 \text{ mJ/m}^2$ , skyrmion formation from the corners to annihilation.



**Fig. 2:** Helicity of skyrmion and antiskyrmion lattice for  $J = 4 \times 10^{11} \text{ A/m}^2$ , 1.0 ns pulse width and  $D = 0.45 \text{ mJ/m}^2$ . **(a)**  $(1, 1, \pi)$  skyrmion, and  $(-1, -1, -\pi/2)$  antiskyrmion. **(b)**  $(1, 1, -\pi/2)$  skyrmion, and  $(-1, -1, 0)$  antiskyrmion. **(c)**  $(1, 1, 0)$  skyrmion and  $(-1, -1, 0)$  antiskyrmion. **(d)**  $(1, 1, \pi/2)$  skyrmion and  $(-1, -1, \pi/2)$  antiskyrmion. The helicity of the skyrmion and antiskyrmions change is due to the field like torque. **(e)** Field like torque variation. Large variation in STT is observed after  $\approx 0.8 \text{ ns}$ .

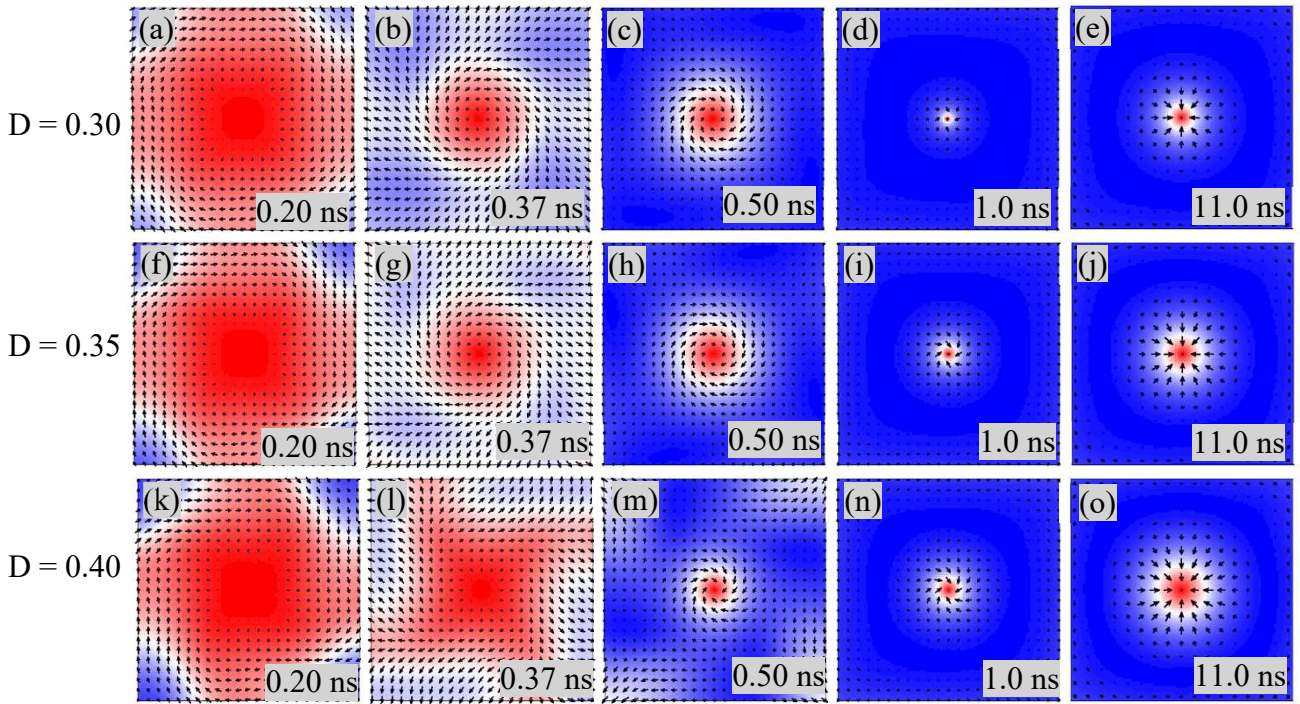


**Fig. 3:** Formation of stable skyrmion for  $J = 5 \times 10^{11} \text{ A/m}^2$  and 1.0 ns pulse width. **(a) – (e)** For  $D = 0.30 \text{ mJ/m}^2$ , **(f) – (j)** are for  $D = 0.35 \text{ mJ/m}^2$  and **(k) – (o)** for  $D = 0.40 \text{ mJ/m}^2$ .

**Movie 1:** Formation of stable skyrmion for  $J = 2 \times 10^{11} \text{ A/m}^2$ , 1.0 ns pulse width and  $D = 0.40 \text{ mJ/m}^2$ . The spin states are shown from 0.0 – 1.0 ns with a step time of 0.01 ns and the final stable skyrmion at 11.0 ns.

**Movie 2:** Formation of skyrmion and antiskyrmion lattice for  $J = 4 \times 10^{11} \text{ A/m}^2$ , 1.0 ns pulse width and  $D = 0.45 \text{ mJ/m}^2$ . The spin states are shown from 0.0 – 1.03 ns with a step time of 0.01 ns.

**Movie 3:** Formation of skyrmion and antiskyrmion lattice for  $J = 4 \times 10^{11} \text{ A/m}^2$ , 1.0 ns pulse width and  $D = 0.50 \text{ mJ/m}^2$ . The spin states are shown from 0.0 – 1.0 ns with a step time of 0.01 ns.

**Movie 4:** Formation of skyrmion and antiskyrmion lattice for  $J = 5 \times 10^{11} \text{ A/m}^2$ , 1.0 ns pulse width and  $D = 0.45 \text{ mJ/m}^2$ . The spin states are shown from 0.0 – 0.60 ns with a step time of 0.01 ns.

**Movie 5:** Formation of skyrmion and antiskyrmion lattice for  $J = 5 \times 10^{11} \text{ A/m}^2$ , 1.0 ns pulse width and  $D = 0.50 \text{ mJ/m}^2$ . The spin states are shown from 0.0 – 1.0 ns with a step time of 0.01 ns.

**Movie 6:** Formation of skyrmion and antiskyrmion lattice for  $J = 4 \times 10^{11} \text{ A/m}^2$ , 0.5 ns pulse width and  $D = 0.45 \text{ mJ/m}^2$ . The spin states are shown from 0.0 – 1.0 ns with a step time of 0.01 ns.

**Movie 7:** Formation of skyrmion and antiskyrmion lattice for  $J = 4 \times 10^{11} \text{ A/m}^2$ , 0.5 ns pulse width and  $D = 0.50 \text{ mJ/m}^2$ . The spin states are shown from 0.0 – 1.0 ns with a step time of 0.01 ns.

**Movie 8:** Formation of skyrmion and antiskyrmion lattice for  $J = 5 \times 10^{11} \text{ A/m}^2$ , 0.5 ns pulse width and  $D = 0.45 \text{ mJ/m}^2$ . The spin states are shown from 0.0 – 3.0 ns with a step time of 0.01 ns.

**Movie 9:** Formation of skyrmion and antiskyrmion lattice for  $J = 5 \times 10^{11} \text{ A/m}^2$ , 0.5 ns pulse width and  $D = 0.50 \text{ mJ/m}^2$ . The spin states are shown from 0.0 – 1.30 ns with a step time of 0.01 ns.

**Movie 10:** Formation of skyrmion lattice and antiskyrmion lattice together for  $J = 5 \times 10^{12} \text{ A/m}^2$ , 0.05 ns pulse width and  $D = 0.35 \text{ mJ/m}^2$ . The spin states are shown from 0.0 – 100 ps with a step time of 1.0 ps.